Corrosion Behavior of Aluminum Alloy in Chloride Media: Electrochemical and Surface Analysis

Mohanad Kadhem Alshujery[1*], Marowah H. Jehad[2]

[1]Ministry of Education, Open Educational College, Department of Science, Baghdad, Iraq

[2]University of Baghdad, College of Science for Women, Department of Chemistry, Baghdad, Iraq

[*]Corresponding Author

DOI: https://doi.org/10.51244/IJRSI.2026.1306000284

Received: 22 June 2026; Accepted: 28 June 2026; Published: 06 July 2026

ABSTRACT

The ziziphus spina-Christi extract (ZSC) was applied as a corrosion inhibitor for aluminum alloy 7051 (A7051) in an acidic medium, 0.1 M HCl. The potentiodynamic polarization measurement was employed to investigate the inhibitor's corrosion inhibition efficiency at various concentrations and different temperatures. The results showed a high inhibition efficiency, up to 95.84% at 7 ppm concentration at a lower examined temperature, indicating effective adsorption of the inhibitor molecule at the aluminium alloy surface.

The polarization data revealed that ZSC acts as a mixed-type corrosion inhibitor be effecting both cathodic reaction (hydrogen evolution) and anodic reaction (metal dissolution). The influence of temperature was examined through Arrhenius and transition state approaches, showing that an increase in activation energy (Ea) occurred after adding ZSC. Adsorption behavior was examined using the Langmuir adsorption isotherm, and the calculated standard free energy of adsorption values confirmed a spontaneous adsorption process dominated by physical interactions.

The inhibition mechanism was attributed to the formation of a protective adsorbed film involving electrostatic interactions and donor–acceptor bonding between ZSC constituents and the A7051 surface. These findings suggest that Ziziphus spina-Christi leaves extract is an effective and environmentally friendly corrosion inhibitor for A7051 in acidic environments.

Keywords: Corrosion, Corrosion inhibitor, Ziziphus spina-Christi, Aluminum alloy

INTRODUCTION

The corrosion of A7051 represents a persistent challenge in numerous industrial applications, including acid pickling, descaling, oil well acidification, and chemical cleaning operations. In acidic environments, particularly hydrochloric acid solutions, A7051 undergoes rapid electrochemical degradation, leading to significant economic losses and safety concerns. Consequently, the development of effective corrosion protection strategies remains a priority in material science and industrial chemistry [1]. Among the available corrosion control methods, the use of corrosion inhibitors is one of the most practical and cost- effective strategies for mitigating metal dissolution under such aggressive conditions. Inhibitors function primarily through adsorption onto the metal surface, forming a protective barrier that reduces the charge transfer process between the metal surface and corrosive medium; however, many conventional synthetic inhibitors exhibit a significant limitation, such as high toxicity, poor biodegradability, and adverse environmental impact. Increasingly stringent environmental regulations have therefore stimulated extensive research into green corrosion inhibitors derived from natural, renewable sources[2].

In recent years, plant-derived extracts have gained considerable attention as green due to their renewable nature and rich chemical composition. Moreover, corrosion inhibitors can be sourced from plants such as flowers,

ISSN No. 2321-2705 | DOI: 10.51244/IJRSI |Volume XIII Issue VI June 2026

seeds, leaves, roots, and stems containing organic compounds such as alkaloids, flavonoids, heteroatoms, tannins, and nitrogen-based compounds. Among them, organic compounds containing heteroatoms are effective corrosion inhibitors. The extracts of these plant parts show good inhibition properties in acidic media. Besides, they are safe, nontoxic, and good for the environment[3].

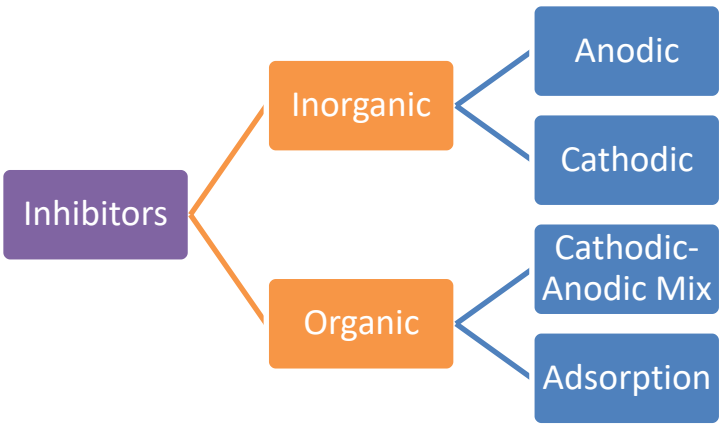

Figure 1: Inhibitors Classification

Ziziphus sphina-Christi leaves are rich in phenolic constituents, including arbutin, flavonoid glycosides, tannins, and chlorogenic acid, which are known for their antioxidant and surface-active properties. Despite their potential, systematic electrochemical investigations addressing the corrosion inhibition behavior of Ziziphus sphina-Christi leaves extracts on A7051 in acidic environments remain limited. Several studies have investigated the corrosion inhibition activity of ZSC leaf extracts. In one study, it was found that a (ZSC) extract inhibited the corrosion of mild steel in acidic media.

The extract was found to be more effective than some synthetic corrosion inhibitors[4, 5]. Therefore, the present work aims to investigate the corrosion inhibition performance of ZSC leaves extracted on A7051 in 0.1 M HCl solution using electrochemical techniques. The inhibition efficiency was evaluated through Potentiodynamic polarization measurements over a range of inhibitor concentration and temperature. Corrosion kinetics parameters were derived from Arrhenius and transition state analysis to assess the effect of temperature on the corrosion isotherm modeling, and the associated thermodynamic parameters were calculated to clarify the nature of inhibitor adsorption. The novelty of this work lies in providing a systematic physical-chemistry-based interpretation of the inhibition mechanism of Ziziphus sphina-Christi leaves extract, combining electrochemical kinetics and adsorption thermodynamics. The findings contribute to the development of effective, low-cost, and environmentally benign corrosion inhibitors for industrial acid applications.

EXPERIMENTAL SECTION

Ziziphus sphina-Christi extracts

A new extraction method, “sonication,” was used in this research. This method has proven effective in shortening the time. Compared to the classical method, where the plant is usually soaked for up to days and extracted by using the Soxhlet apparatus several times[6-8]. This ultrasound-assisted extraction not only reduces extraction times but also the volume of extractant. ZSC leaves were collected from Dora (Arab-Jabour), a neighborhood immediately south-east of Baghdad that lies to the west of the Tigris River of Baghdad, Iraq.

The collected leaves were dried in the air and then ground into powder. One hundred grams of ZSC leaves were added to 200 mL of ethanol in the bottom flask, which was then continuously sonicated for 1 hour at 80 kHz using a Power Sonic 405. The mixture was then filtered and dried using a rotary evaporator. 1 g of green powder was obtained (1 % yield). The prepared dried ZSC leaves extract is readily soluble in water, methanol, and ethanol. A stock solution of 10,000 ppm ZSC extract was prepared by dissolving 250 mg extract in 25 mL

ISSN No. 2321-2705 | DOI: 10.51244/IJRSI |Volume XIII Issue VI June 2026

deionized water. To prepare the low concentration of ZSC for the inhibition experiment, an intermediate solution of 100 ppm was first prepared by diluting 1 mL of the 10000-ppm solution to 100 mL using deionized water. In the inhibition of A7051 experiments, aliquots from this stock solution were used to prepare diluted ZSC solutions of concentrations (1, 5, 7, and 10 ppm) in HCl (0.1 M) medium[9].

Figure 2: crushed Ziziphus sphina-Christi leaves.

Preparation of electrode samples

Table 1 shows the chemical composition of A7051 that was used. The working electrode samples used in dimensional polarization experiments (2×2cm) have a thickness of 4 mm. The A7051 sample was regularly polished with different SiC paper grades (between 400 – 2500) mesh, after cleaning; the polished Instances of distilled water, ethanol, and acetone were dried, then desiccated. Only 1 cm^2 of the working electrode was exposed to a corrosive solution in the polarization analysis, using the electrode holder of the corrosion experiment [10, 11].

Table 1: Chemical composition of A7051

Al	**Zn**	**Mg**	**Mn**	**Cr**	**Fe**	**Si**	**Cu**	**Ti**
92%	3%	2.5 %	0.045%	0.25 %	0.045 %	0.35%	0.15%	0.15 %

Corrosion cell

The Pyrex Corrosion cell with (1L) consists of two containers, internal and external. The water bath was used to control the temperature of 0.1 M HCl, which flows into the external container at (298, 308, 318, and 328) K.

The corrosion cell, three electrodes, and the thermostat are placed in the internal container.

The three electrodes can be explained as follows:

1. The Reference Electrodes (R.E) were used in this study to estimate the W.E potential according to the potential of the R.E. The R.E potential is well known and accurate, and it is combined with two tubes; the internal tube contains AgCl, Ag, and KCl. The outer tube is filled with the prepared artificial saliva solution. The reference electrode is placed 2 mm from the working electrode to reduce IR drop.
2. The Auxiliary Electrode (A.E) is made of platinum (high purity); its length is approx. about (10 cm).
3. Working Electrode (W.E) is testing treated A7051, whose potential will be measured.

The A7051 is inserted in the holder in which the diameter of the exposed surface to the 0.1M HCl is ($1cm^2$). The complete polarization measurement system is shown in Figure 3. In this study, we chose 0.1 M HCl to avoid the problems linked to the ohmic drop. Every 1 ml from the 100-ppm solution represents 1 ppm. So, adding 1, 5, 7, and 10 ml to 999, 995, 993 and 990 ml of blank solution. However, the acid medium represents HCl 0.1 M. By dilution, the blank and 1, 5, 7, and 10 ml of the extraction solution were added to 999, 995, 993, and 990 ml of the blank solution.

ISSN No. 2321-2705 | DOI: 10.51244/IJRSI |Volume XIII Issue VI June 2026

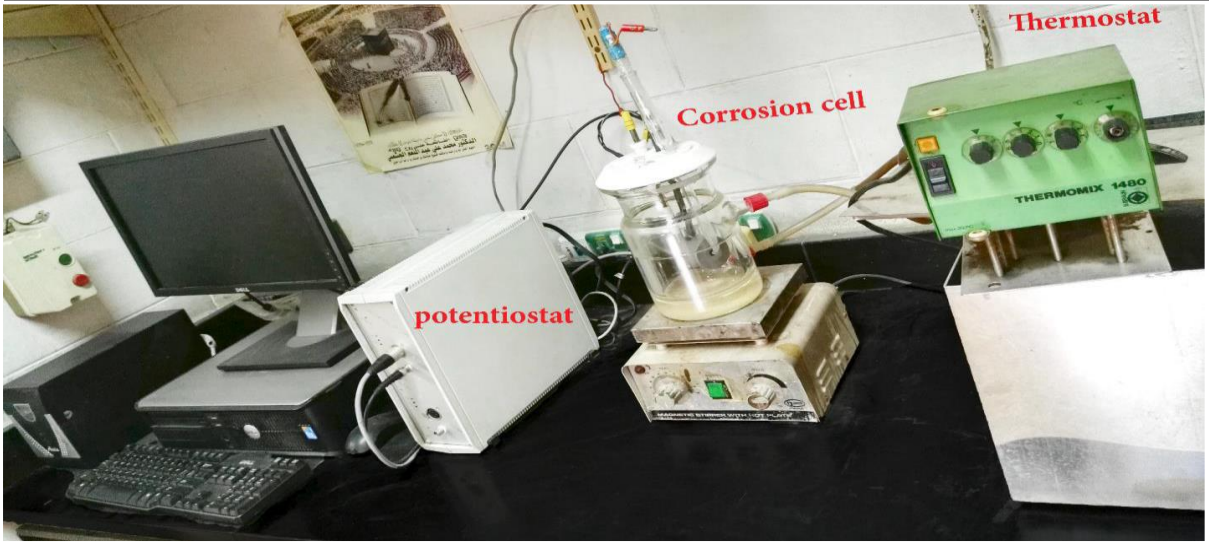

Figure 3: Full system is set up for measuring polarization.

Corrosion Tests and Inhibition Efficiency

The potentiostat MLabSci (Germany, 2000) has been used for electrochemical tests and controlled by MLabSci software at a temperature range of 298-328 K. Three electrodes had been used in the corrosion cell, silver-silver chloride used as a reference electrode.

In contrast, an auxiliary electrode and its platinum electrode with (1 cm^2) surface area of the working electrode was A7051. The final corrosive solutions (saline solution and inhibitor solution, acid solution and inhibitor solution). At each experiment onset, the working electrode must be immersed in the corrosive solution (uninhibited and inhibited) to get the stabilization state. The MLabSci software was used to calculate the parameters from Tafel polarization (corrosion potential E_{Corr}, cathodic b_c and anodic b_a, and a current density of corrosion I_{Corr})[12].

RESULTS AND DISCUSSION

Potentiodynamic Polarization

Figure 4 illustrates the Potentiodynamic polarization curves of A7051 in 0.1 M HCl solutions in the absence and presence of various concentrations of Ziziphus sphina-Christi leaves extract (ZSC) at a temperature ranging from 298 to 328 K. The corresponding electrochemical kinetics parameters are summarized in Table 2.

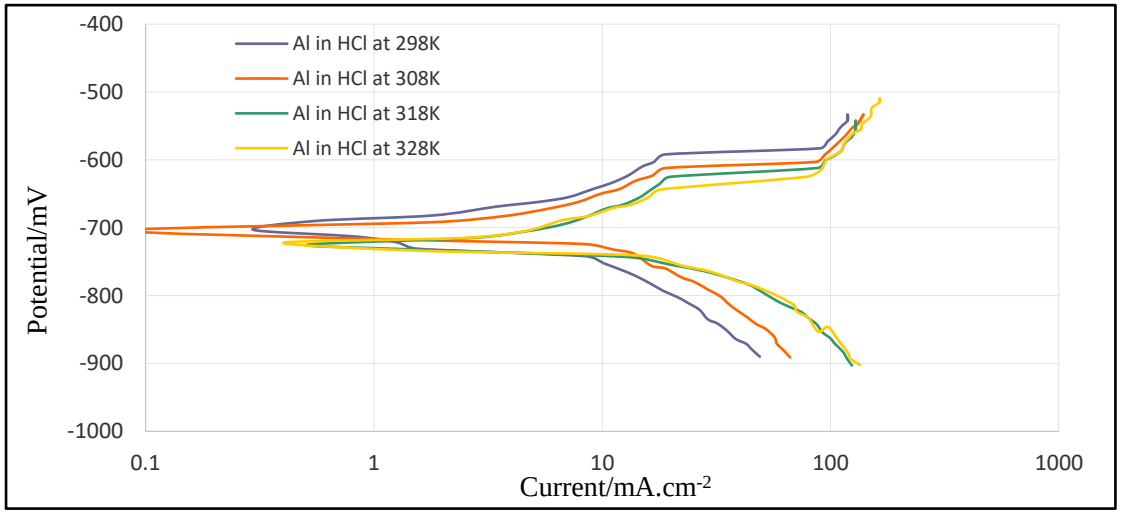

Figure 4: The polarization curve of A7051 in 0.1 HCl without inhibitor and with different concentrations of inhibitor

ISSN No. 2321-2705 | DOI: 10.51244/IJRSI |Volume XIII Issue VI June 2026

In the uninhibited solution, the corrosion current density (I_{Corr}) increased with increasing temperature, reflecting the thermally activated nature of the corrosion process. Upon the addition of ZSC, a significant decrease in I_{Corr} was observed at all studied temperatures, indicating the effective inhibition of A7051 corrosion.

The shift in corrosion Potential (E_{Corr}) upon inhibitor addition was less than 85 mV in acidic medium, suggesting the ZSC acts predominantly as a mixed-type inhibitor, suppressing both anodic metal dissolution and cathodic hydrogen evolution reactions. This behavior implies that the inhibitor molecules adsorb fundamental reaction mechanisms.

The relatively unchanged anodic (ba) and cathodic (bc) Tafel slopes in the presence of ZSC further support this conclusion, indicating that corrosion inhibition occurs mainly through surface coverage rather than modification of reaction kinetics. The inhibition efficiency (%IE), calculated from corrosion current densities, increased with inhibitor concentration and reached a maximum at 7 ppm, demonstrating the formation of a stable protective adsorbed film on the A7051 surface. Notably, the inhibition efficiency remained relatively constant with temperature, suggesting a strong interaction between inhibitor molecules and the metal surface. These values were calculated using the following equation [1]:

where $I°_{Corr}$ and I_{Corr} are the corrosion rate in the absence and presence of ZSC, respectively[9].

$$\text{IE\%} = \frac{Icorr° - Icorr}{Icorr°} - \text{x } 100$$

Table 2: Corrosion kinetic parameters for *Ziziphus sphina-Christi* leaves in 0.1 M HCl at the temperature range (298-328) K.

	Temp. (K)	E_{Corr} (mV)	I_{Corr} ($\mu A.cm^{-2}$)	-bc	Ba	R_p	IE%
Blank	298	-741	5.05	405.6	44.3	3.4	
	308	-768	7.8	216	33.6	1.9	
	318	-792	7.75	317.4	37.3	1.8	
	328	-809	11.29	211.1	45.1	1.4	
1 ppm	298	-712	0.43	56.9	20.6	6.4	91.49
	308	-774	1.28	63.1	73.6	5.1	83.59
	318	-806	1.3	121.4	70.4	4.5	83.23
	328	-827	3.7	82.1	73.3	3.1	67.23
5 ppm	298	-667	0.39	156	188.4	5.2	92.28
	308	-729	1.1	145.3	100.8	3.5	85.9
	318	-818	1.2	68.3	227.9	3.2	84.52
	328	-853	1.9	101.1	138.9	1.9	83.17
7 ppm	298	-723	0.21	71	52.7	8.2	95.84
	308	-751	0.71	204	57.7	7.6	90.9
	318	-798	0.81	89.4	66.2	4.1	89.55
	328	-832	1.39	131.2	52.8	3.1	87.69
10 ppm	298	-508	0.54	108.8	56	9.1	89.31
	308	-606	1.32	108.2	61.3	7.4	83.08
	318	-612	1.51	157.5	61.5	5.8	80.52
	328	-631	2.3	85.8	42.7	3.9	79.63

ISSN No. 2321-2705 | DOI: 10.51244/IJRSI |Volume XIII Issue VI June 2026

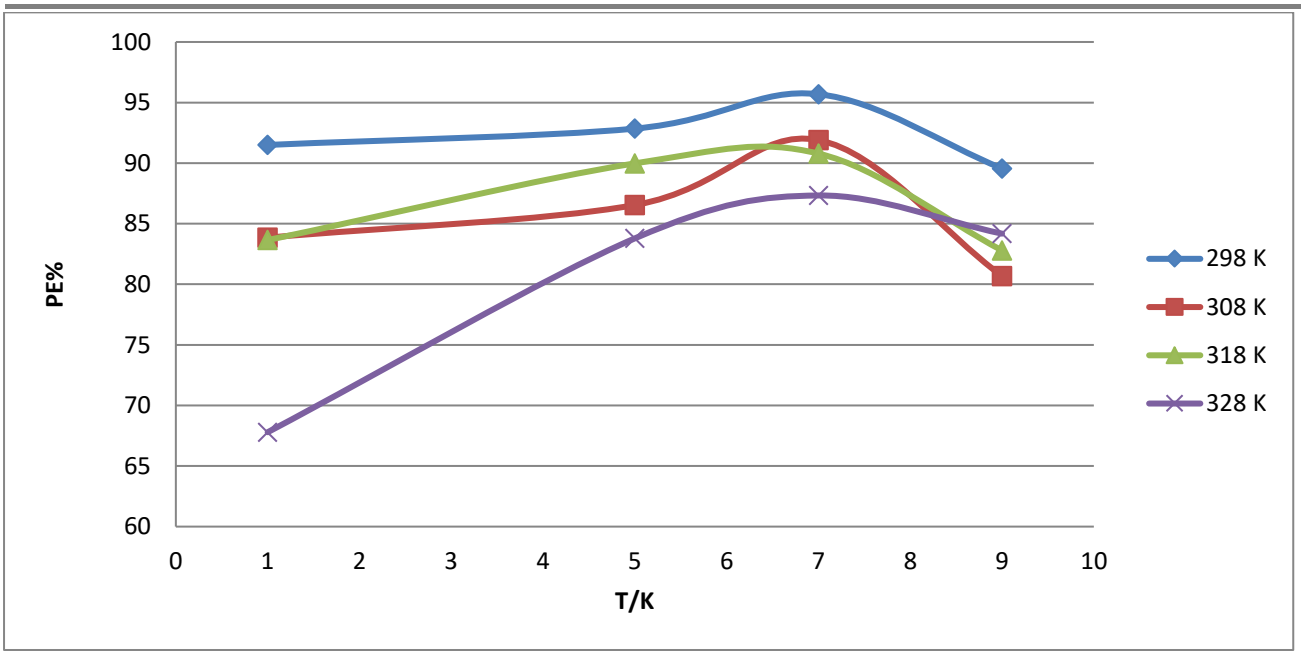

Figure 5: The relation between inhibitor efficiency (IE%) and temperature with inhibitors concentration in 0.1 M HCl.

The protection efficiency did not affect with temperature, indicating the stability of adsorbed layer on metal surface. Based on the Stern–Geary equation, small polarization near the corrosion potential is performed to determine corrosion resistance[13]:

$$\text{Rp} = \frac{\mathbf{ba\ bc}}{\mathbf{2.303\ (ba + bc)}^{\circ}} \text{ x } \frac{1}{\text{Icorr}}$$

Effect of temperature and kinetic parameters.

The effect of temperature on the corrosion behavior of A7051 in 0.1 M HCl solution in the absence and presence of Ziziphus sphina-Christi leaves extract (ZSC) was evaluated in the temperature range of 298- 328 K. As shown by the Potentiodynamic polarization results, the corrosion current density (I_{Corr}) increased with increasing temperature for both uninhibited and inhibited systems, confirming the thermally activated nature of the corrosion process.

The kinetic parameters were evaluated using the Arrhenius equation[14, 15]:

$$\text{Log } Icorr = \frac{-Ea}{2.303\ \text{RT}} + \text{Log A}$$

And the transition state equation:

$$\text{Log } (\frac{Icorr}{\text{T}}) = \log (\frac{R}{\text{Nh}}) + \frac{\Delta S*}{2.303\ \text{R}} - \frac{\Delta H*}{2.303\ \text{RT}}$$

where Ea represents the activation energy of the corrosion process, R is the gas constant (R = 8.314 J K^{-1} mol^{-1}), A is the pre-exponential factor, h is Planck's constant (6.626176 $\times 10^{-34}$ Js) , N is Avogadro's number (6.022×1023 mol^{-1}), ΔS^* is the entropy of activation, and ΔH^* is the enthalpy of activation[9]. The Arrhenius plots (log I_{Corr} vs. $1/T$) exhibited good linearity, indicating that the corrosion process follows Arrhenius behavior. The calculated kinetic parameters are summarized in Table 3.

The values of activation energy in the presence of ZSC were higher than those obtained for the uninhibited solution, this increasing in Ea. Suggest that the adsorption of ZSC molecules hides the charge transfer process at the metal-solution interface by forming a protective surface film.

ISSN No. 2321-2705 | DOI: 10.51244/IJRSI |Volume XIII Issue VI June 2026

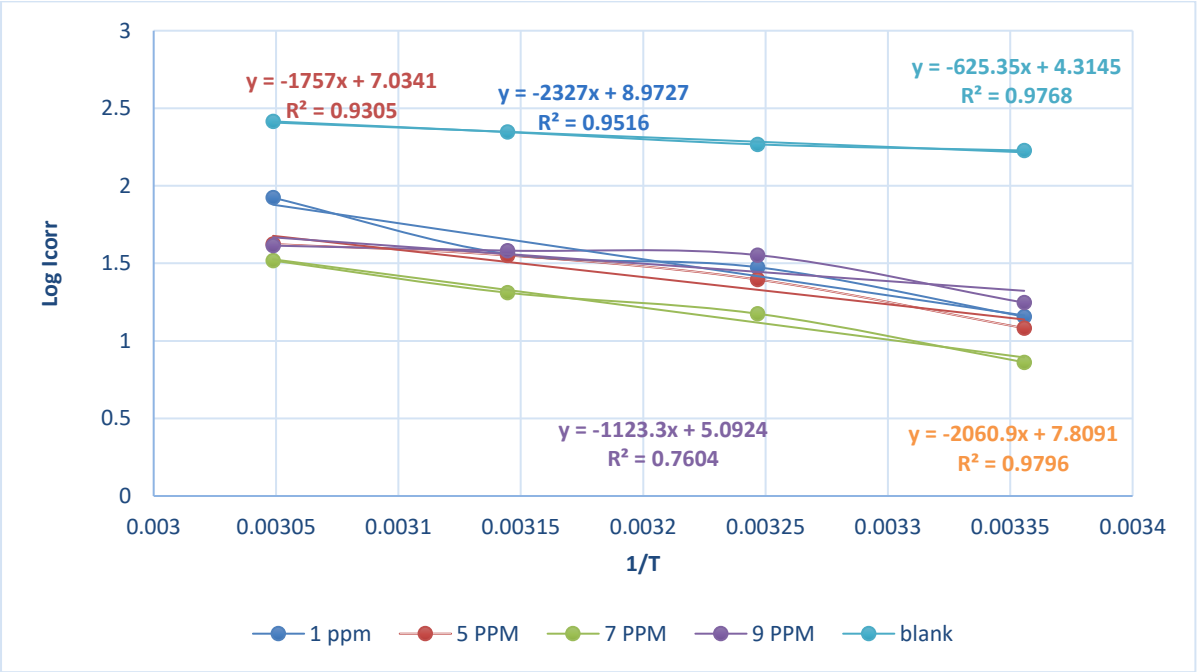

Figure 6: *Arrhenius Plot of logicorr Versus 1/T for the corrosion of A7051 0.1 M HCL solution in the absence and presence of various* Ziziphus sphina-Christi leaves *concentrations***.**

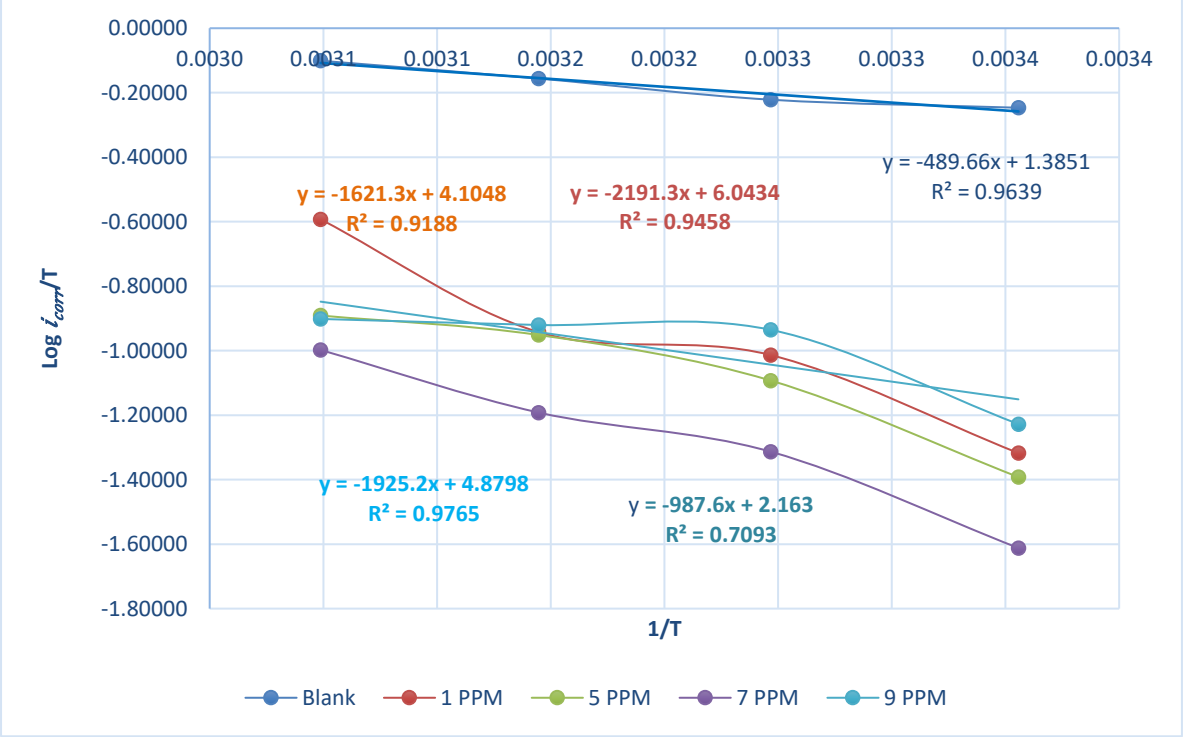

Figure 7: *log icorr/T* Versus 1/T for the corrosion of Ziziphus sphina-Christi leaves in 0.1 M HCL solution in the absence and presence of various (ZSC) concentrations**.**

As shown in Table 3. the positive values of activation enthalpy (ΔH^*) indicate the endothermic nature of the corrosion process, while the negative values of activation entropy (ΔS^*) reflect a decrease in disorder during the formation of the activated complex, consistent with an associative adsorption mechanism, in which inhibitor molecule replace water molecule adsorbed on the metal surface, leading to more ordered transition state.

ΔH*value for the transition state of corrosion for A7051 in 0.1M HCl medium increases after being inhibited by ZSC. The highest ΔH* value occurred with (1,5,7) ppm of ZSC. However, the entropy of activation value

ISSN No. 2321-2705 | DOI: 10.51244/IJRSI |Volume XIII Issue VI June 2026

ΔS* for the corrosion of A7051 in 0.1M HCl solutions was slightly affected when ZSC was added to the corrosive solution.

Table 3: The thermodynamic parameter Ziziphus sphina-Christi leaves in 0.1 M HCL

C_{inh}	ΔH*/kJ.mol^{-1}	ΔS*/J.K^{-1}.mol^{-1}	Ea/kJ.mol^{-1}	A/Molecule Cm^{-1}S^{-1}
Blank	9.375	-0.171	11.97	1.24E+28
1 PPM	41.957	-0.081	44.56	5.65E+32
5 PPM	31.043	-0.119	33.64	6.51E+30
7 PPM	36.862	-0.104	39.46	3.88 E+31
10 PPM	18.909	-0.156	21.51	7.45 E+28

Adsorption Isotherm and Adsorption Thermodynamics

The corrosion inhibition behavior of Ziziphus sphina-Christi leaves extract is primarily governed by the adsorption of its bioactive constituents onto the A7051 surface. To elucidate the nature of this adsorption process, the surface coverage ($\boldsymbol{\theta}$) values were calculated from inhibition efficiency data according to:

$$\boldsymbol{\theta} = \frac{\boldsymbol{IE}\%}{\mathbf{100}}$$

Several adsorption isotherm models were examined, and experimental data were found to fit the Langmuir adsorption isotherm, which can be expressed as:

$$\frac{C_{inh}}{\boldsymbol{\theta}} = \frac{\mathbf{1}}{K_{ads}} + C_{inh}$$

where C_{inh} Is the inhibitor concentration and K_{ads} is the adsorption equilibrium constant. The linear relationship obtained by plotting $\frac{C_{inh}}{\theta}$ versus C_{inh} A slope close to unity confirms the applicability of the Langmuir model, suggesting monolayer adsorption of ZSC molecules on a homogeneous A7051 surface.

Thermodynamic function for the adsorption process (ΔH_{ads}, ΔS_{ads}. ΔG_{ads}) can be calculated using the known formulas [16]:

$$K_{ads} = \frac{1}{55.5} \exp\left[\frac{-\Delta G_{ads}}{RT}\right]$$

This equation can also be expressed as:

$$\Delta G_{ads} = -2.303RT\log(55.5K_{ads})$$

Assuming the thermodynamic model, corrosion inhibition of A7051 in the presence of (ZSC) can be better explained using the enthalpy of adsorption $\Delta H_{ads,}$ and entropy of adsorption $\Delta S_{ads,}$ which can be calculated from the integrated Van't Hoff equation:

$$\log K_{ads} = \frac{-\Delta H_{ads}}{2.303RT} + \frac{\Delta S_{ads}}{2.303R} + \log\frac{1}{55.5}$$

To calculate the enthalpy of adsorption and entropy of adsorption, logKads was plotted against 1/T, and a straight line was obtained with slope equal to ($-\Delta H_{ads}/2.303R$) and intercept equal to ($\Delta S_{ads}/2.303R+\log 1/55.5$). The calculated values of the heat of adsorption and entropy of adsorption are listed in Table 4. where 55.5 represents the molar concentration of water in the solution. The calculated values of ΔG°_{ads}were negative, indicating a spontaneous adsorption process. The magnitude of $\Delta G^{\circ}_{ads}$was found to be in the range typically associated with physical adsorption, suggesting that electrostatic interactions between protonated inhibitor molecules and the charged metal surface play a dominant role. However, the relatively high inhibition

ISSN No. 2321-2705 | DOI: 10.51244/IJRSI |Volume XIII Issue VI June 2026

efficiency and its weak dependence on temperature indicate that specific chemical interactions may also contribute to the adsorption process.

The adsorption of ZSC constituents on the A7051 surface can be attributed to the presence of multiple oxygen-containing functional groups, aromatic rings, and π-electrons in phenolic and flavonoid compounds. These groups can interact with vacant iron d-orbitals through donor–acceptor interactions, while competitive adsorption with chloride ions further stabilizes the protective adsorbed layer.

Overall, the adsorption isotherm and thermodynamic analyses confirm that the corrosion inhibition of A7051 by Ziziphus sphina-Christi leaves extract proceeds via spontaneous adsorption, forming a stable and compact protective film that effectively suppresses both anodic and cathodic corrosion reactions.

Table 4: The adsorption parameter for Ziziphus sphina-Christi leaves in 0.1 M HCL at the temperatures range (298-328) K.

	Temp.	K_{ads}	ΔG_{ads}/ kJ.mol^{-1}	$-\Delta S_{ads}$/ J.K^{-1}.mol^{-1}	$-\Delta H_{ads}$/ kJ.mol^{-1}
ZSC Inhibitor	298	10.549	-15.793	-34.6508	-25.7931
	308	5.043	-13.964		
	318	5.522	-14.189		
	328	3.575	-13.112		

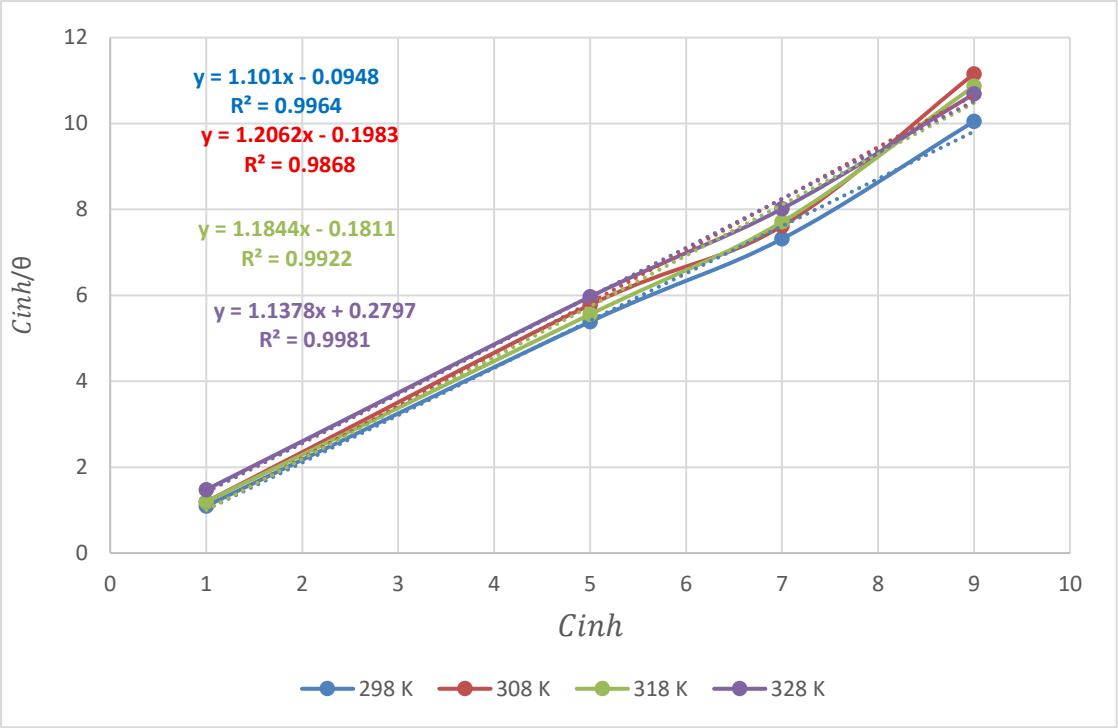

Figure 8: Langmuir isotherm plot for the adsorption of Ziziphus sphina-Christi leaves in 0.1 M HCL solution in the presence of various (ZSC) concentrations

Mechanism of Corrosion Inhibition by Ziziphus sphina-Christi Leaves Extract

The corrosion inhibition of A7051 in 0.1 M HCl solution by Ziziphus sphina-Christi leaves extract (ZSC) can be attributed to the adsorption of its bioactive constituents onto the metal surface, resulting in the formation of a protective interfacial film. The inhibition mechanism involves a combination of electrostatic interactions and specific donor–acceptor interactions, consistent with the electrochemical, kinetic, and adsorption thermodynamic findings.

In acidic media, A7051 surfaces become positively charged due to the adsorption of hydrogen ions, while chloride ions are strongly adsorbed onto the metal surface, creating locally negatively charged sites. In this

ISSN No. 2321-2705 | DOI: 10.51244/IJRSI |Volume XIII Issue VI June 2026

environment, ZSC constituents—many of which are protonated—can adsorb onto the steel surface through electrostatic attraction with adsorbed chloride ions, facilitating physical adsorption. This interaction is supported by the negative values of the standard free energy of adsorption and the observed decrease in inhibition efficiency with increasing temperature.

In addition to electrostatic interactions, the molecular structure of ZSC constituents plays a crucial role in the inhibition process. The presence of multiple oxygen-containing functional groups (such as hydroxyl and carbonyl groups), aromatic rings, and π-electrons enable specific chemical interactions with the metal surface. These functional groups can donate electron density to the vacant d-orbitals of iron atoms, leading to the formation of coordinate bonds that enhance the stability of the adsorbed layer. Such donor–acceptor interactions contribute to the high inhibition efficiency observed even at low inhibitor concentrations.

The mixed-type inhibition behavior observed in Potentiodynamic polarization measurements indicates that ZSC suppresses both anodic metal dissolution and cathodic hydrogen evolution reactions. This dual action suggests that the adsorbed inhibitor film uniformly covers active anodic and cathodic sites on the A7051 surface, thereby reducing charge transfer across the metal–solution interface.

Furthermore, the increase in activation energy in the presence of ZSC confirms that the inhibitor increases the energy barrier for the corrosion reaction, while the decrease in activation entropy reflects a more ordered system during the formation of the activated complex. These kinetic features are consistent with the formation of a compact and adherent protective film that restricts the mobility of reactive species at the interface.

Overall, the corrosion inhibition mechanism of Ziziphus sphina-Christi leaves extract involves spontaneous adsorption driven predominantly by physical interactions, reinforced by localized chemical bonding. The synergistic effect of these interactions results in the formation of a stable protective layer that effectively mitigates the corrosion of A7051 in acidic environments.

FE-SEM Study

The FESEM techniques showed the morphology of the inhibitor layer absorbed on the A7051 substrate. Figure 9 shows the topographical baseline of the aluminum before the inhibition process in the absence of ZSC and aggressive medium. As shown in the figure, a very uniform and flat surface of A7051 was observed, with unidirectional micro-striations, which are typical residual artifacts from the silicon carbide polishing process [17].

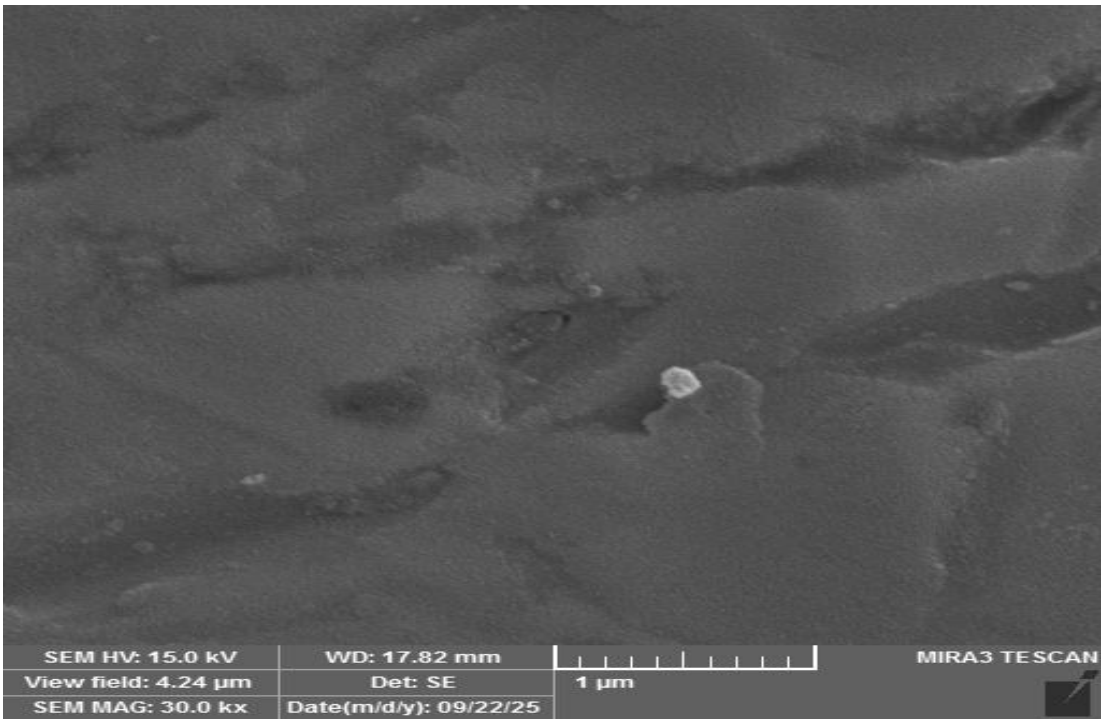

Figure 9: FESEM Image of the Polished A7051 Surface before Acid Exposure.

ISSN No. 2321-2705 | DOI: 10.51244/IJRSI |Volume XIII Issue VI June 2026

After putting the A7051 in the corrosive media, significant morphological scratching and damage was shown, a highly irregular, porous surface, and surface pitting and cavities in A7051 substrate surface as shown in Figure 10. This damage is caused by the high activity of hydronium and chloride ions at the A7051-electrolyte interface[18].

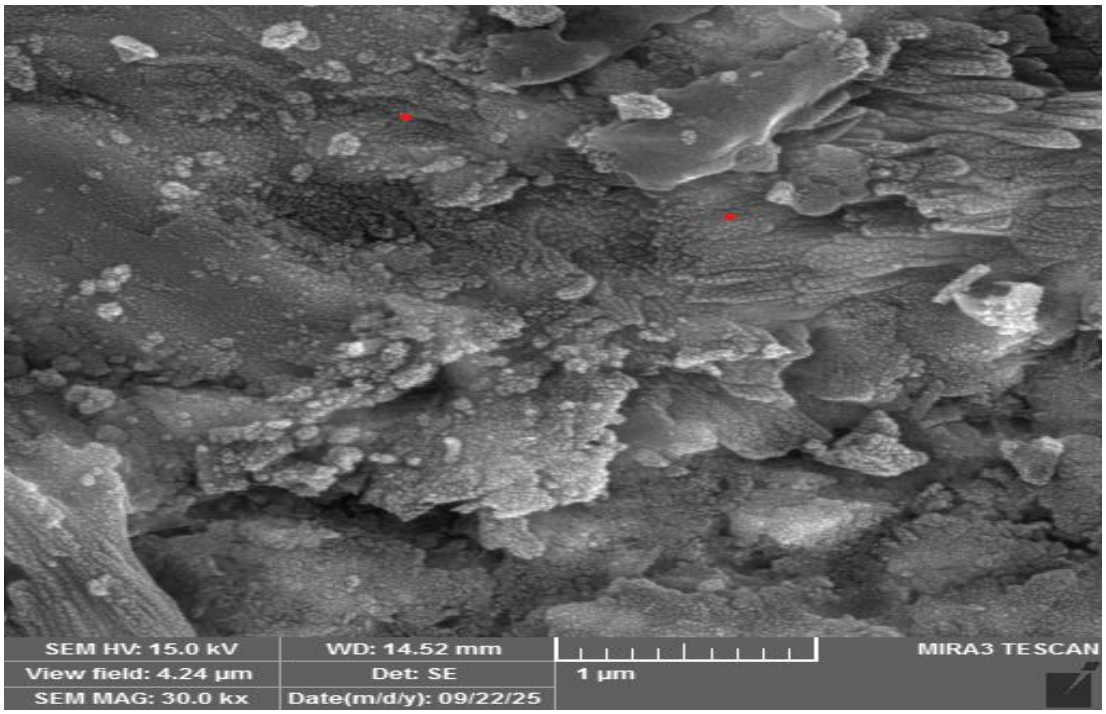

Figure 10: FESEM Image of the A7051 Surface after Immersion in the Uninhibited 0.1 M HCl Solution.

After adding ZSC, the FESEM image (Figure 11) shows a good change on the A7051 surface, the pitting and porous are eliminated, and a passivation layer is formed which confirms the interfacial coordination of ZSC with A7051 surface yielding highly stable metal-organic complexes. [19, 20]. thereby effectively blocking both the anodic dissolution and cathodic reaction pathways[21] .

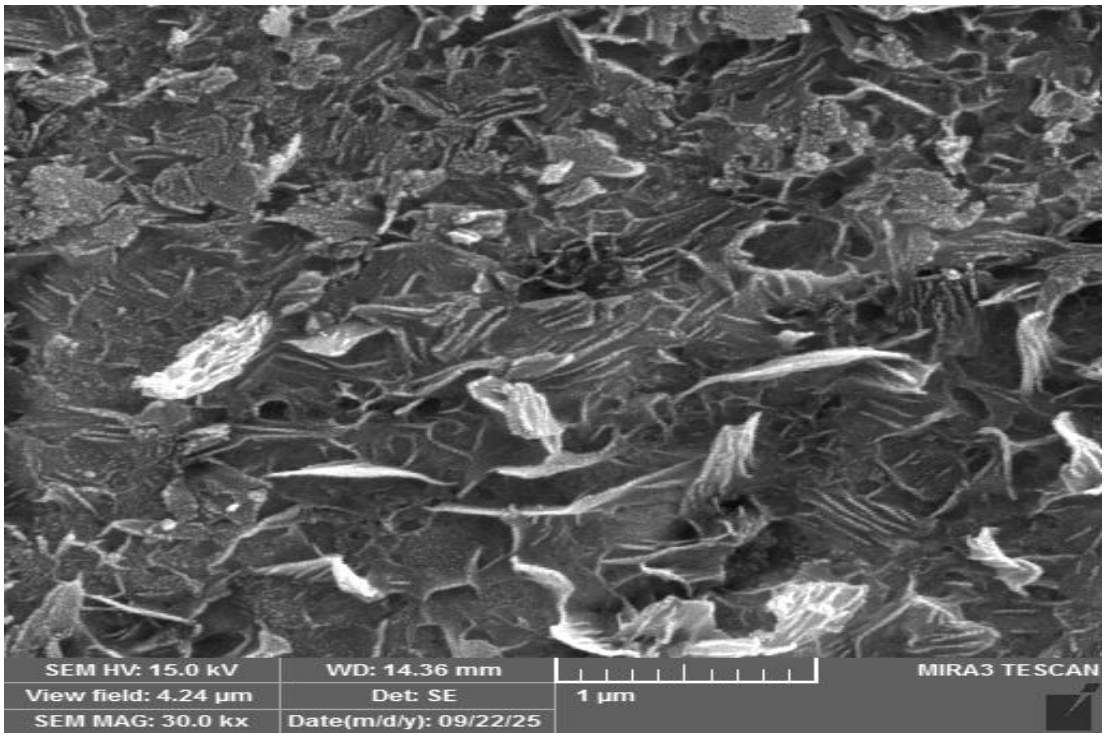

Figure 11: FESEM Image of the A7051 Surface after Immersion in a 0.1 M HCl Containing the Optimal Concentration of ZSC Extract Medium after Adding the Inhibitor

ISSN No. 2321-2705 | DOI: 10.51244/IJRSI |Volume XIII Issue VI June 2026

CONCLUSION

Ziziphus sphina-Christi leaves extract demonstrated excellent corrosion inhibition performance for A7051 in 0.1 M HCl solution. The inhibition efficiency increased with inhibitor concentration and reached a maximum at 7 ppm.

Potentiodynamic polarization results revealed that the extract acts as a mixed-type inhibitor, reducing both anodic and cathodic reactions primarily through surface adsorption. Kinetic and thermodynamic analyses indicated that the presence of the extract increases the activation energy and enthalpy of corrosion, confirming the formation of a protective adsorbed layer on the A7051 surface. The relatively stable inhibition efficiency with increasing temperature suggests a strong interaction between the bioactive constituents of the extract and the metal surface. Overall, Ziziphus sphina-Christi leaves extract can be considered a promising eco-friendly corrosion inhibitor for A7051 in acidic environments.

REFERENCES

1. Kamil, F.H., et al., *Corrosion Behaviour, Kinetic and Thermodynamic Studies of Water Hyacinth Extract as a Corrosion Inhibitor for Low-Carbon Steel.* Iraqi Journal of Industrial Research, 2024. **11**(3): p. 35-44.
2. Kadhim, A., et al., *Corrosion inhibitors. A review.* International Journal of Corrosion and Scale Inhibition, 2021. **10**(1): p. 54-67.
3. Hossain, N., M. Asaduzzaman Chowdhury, and M. Kchaou, *An overview of green corrosion inhibitors for sustainable and environment friendly industrial development.* Journal of Adhesion Science and Technology, 2021. **35**(7): p. 673-690.
4. Natarajan, R. and F.S.Z.S. Al Shibli, *Synthesis of biomass derived product from Ziziphus spina-christi and application for surface protection of metal under acidic environment-Performance evaluation and thermodynamic studies.* Chemosphere, 2021. **284**: p. 131375.
5. Shahryari, Z. and K. Gheisari, *Corrosion inhibition properties of Ziziphus spina-christi leaves extract and zinc cations on mild steel in sodium chloride solution.* Materials Chemistry and Physics, 2023. **299**: p. 127474.
6. Al-Ashoor, S.Z., D.S. Ali, and H.Z. Al-Sawaad, *Ziziphus spina Christi leaves methanol extract evaluation as antifungal, antibacterial, antioxidant and green inhibitor for carbon steel alloy corrosion in hydrochloric acid.* Portugaliae Electrochimica Acta, 2023. **41**(2): p. 167-184.
7. Sargenti, S.R. and W. Vichnewski, *Sonication and liquid chromatography as a rapid technique for extraction and fractionation of plant material.* Phytochemical Analysis: An International Journal of Plant Chemical and Biochemical Techniques, 2000. **11**(2): p. 69-73.
8. Yeasmen, N. and V. Orsat, *Pulsed ultrasound assisted extraction of alternative plant protein from sugar maple leaves: Characterization of physical, structural, thermal, electrical, and techno-functional properties.* Food Hydrocolloids, 2024. **152**: p. 109960.
9. Al-Mashhadani, H.A., et al. *Anti-corrosive substance as green inhibitor for carbon steel in saline and acidic media*. in *Journal of Physics: Conference Series*. 2021. IOP Publishing.
10. Jehad, M.H., et al., *Anodizing of pure aluminum alloy with incorporated ferric oxide nanoparticles to enhance the aluminum corrosion resistance.* Research Journal of Pharmacy and Technology, 2023. **16**(6): p. 2935-2940.
11. Alshujery, M.K. and K.A.S. Al-Saadie. *Corrosion inhibition of aluminum 6061 alloy by a micro arc oxidation modified with incorporated zinc oxide nanoparticles*. in *4TH INTERNATIONAL SCIENTIFIC CONFERENCE OF ENGINEERING SCIENCES AND ADVANCES TECHNOLOGIES*. 2023. AIP Publishing LLC.
12. Mohammed, R. and H. Almashhadani, *Synthesis, characterization and thermodynamic study of a polymer nanocomposite from methyl acrylate and zirconium chloride as an anti-corrosion coating for carbon steel.* Int. J. Corros. Scale Inhib, 2023. **12**(3): p. 1180-1191.
13. Vera, J., K. Evans, and C. Mendez. *Derivation of a Modified Stern-Geary Linear Polarization Equation. Application to seawater corrosion and inhibitor evaluation*. in *CONFERENCE 2024*. 2024. Association for Materials Protection and Performance.

14. Koga, N., *A review of the mutual dependence of Arrhenius parameters evaluated by the thermoanalytical study of solid-state reactions: the kinetic compensation effect.* Thermochimica acta, 1994. **244**: p. 1-20.
15. Mahmmod, A.A., et al., *Quinoxaline as a corrosion inhibitor for copper in nitric acid: Kinetics, statistical, and theoretical investigations.* Case Studies in Chemical and Environmental Engineering, 2024. **10**: p. 100836.
16. de Lima, A.C.A., et al., *Adsorption Thermodynamics*, in *Adsorption*. CRC Press. p. 76-110.
17. Nandee, R., et al., *Surface topography and surface morphology of graphene nanocomposite by FESEM, EDX and AFM analysis.* Nano-Structures & Nano-Objects, 2024. **38**: p. 101170.
18. Kairi, N.I. and J. Kassim, *The effect of temperature on the corrosion inhibition of mild steel in 1 M HCl solution by Curcuma longa extract.* International Journal of Electrochemical Science, 2013. **8**(5): p. 7138-7155.
19. Alshujerya, M.K. and K.A.S. Al-Saadiea, *Aluminum 6061 Alloy Modification with Micro Arc Oxidation and Ferric Oxide Nanoparticles Incorporated to Reduce Aluminum Corrosion.* Egyptian Journal of Chemistry, 2023. **66**(5): p. 99-105.
20. Holla, B.R., et al., *Plant extracts as green corrosion inhibitors for different kinds of steel: A review.* Heliyon, 2024. **10**(14).
21. Shathani, P., et al., *Plant leaves extracts as green corrosion inhibitors of steel in acidic and seawater environments: a review.* Environmental Science and Pollution Research, 2025: p. 1-22.